ADVANCED FUNCTIONAL MATERIALS
www.afm-journal.de

Dramatic Enhancement of Photoluminescence Quantum Yields for Surface-Engineered Si Nanocrystals within the Solar Spectrum

Vladimir Svrcek, Katerina Dohnalova, Davide Mariotti, Minh Tuan Trinh, Rens Limpens, Somak Mitra, Tom Gregorkiewicz, Koiji Matsubara, and Michio Kondo*

Substantial improvements of the absolute photoluminescence quantum yield (QY) for surfactant-free silicon nanocrystals (Si-ncs) by atmospheric pressure microplasma 3-dimensional surface engineering are reported. The effect of surface characteristics on carrier multiplication mechanisms is explored using transient induced absorption and photoluminescence QY. Surface engineering of Si-ncs is demonstrated to lead to more than 120 times increase in the absolute QY (from 0.1% up to 12%) within an important spectral range of the solar emission (2.3–3 eV). The Si-ncs QY is shown to be stable when Si-ncs are stored in ethanol at ambient conditions for three months.

1. Introduction

In the last decades, considerable progress has been made in the synthesis, manipulation, and device integration of nanoscale objects for a range of applications.[1–5] While experimental research has given the opportunity to verify theoretical predictions, nanoscale material engineering has also evolved into suggesting an even wider range of exciting opportunities.[6–8] Nanomaterials and interface engineering at the nano- or atomic-scale[9–11] can contribute to the development of advanced devices with new physical phenomena and superior performance for a variety of applications in medicine, electronics, or photovoltaics (PV), and so forth.

The use of nanostructured silicon, and in particular the use of silicon nanocrystals (Si-ncs) with quantum confinement, offers important additional advantages over other nanoscale materials. Firstly, elemental silicon is non-toxic, with a limited environmental footprint and an established infrastructure for both the supply of raw materials and for large scale manufacturing.[12] Secondly, Si-ncs belong to a class of materials that undergo key changes when scaled down to dimensions below the Bohr radius (e.g., quantum confinement[13]). Furthermore, the interplay between quantum confinement effects and surface effects is particularly important in covalent semiconductors, as Si, with potential new opportunities for tailoring Si-ncs characteristics.[14,15] Amongst the various resulting nanoscale properties, enhanced carrier multiplication (CM) has been the center of recent and vigorous research activities and highly efficient CM in Si-ncs has been reported. It has been demonstrated that PV devices could greatly benefit from CM in Si-ncs.[16–18] Therefore, the prospects offered by Si-ncs are highly relevant for PVs, and could lead to highly efficient solar cells exceeding Shockley-Queisser limit.[19,20] However, the understanding and control of CM mechanisms in Si-ncs and the role of the surface states is still limited, and the related experimental results are debated.[21–25]

In order to achieve a successful PV technology based on Si-ncs with CM, high concentrations of closely-packed Si-ncs is fundamentally important,[6,26] and the use of stable Si-ncs colloids could represent a potential methodology meeting the necessary processing requirements,[10] such as cheap "printing", "stamping", "spraying", or roll-to-roll technologies.

Given the crucial role played by the surface chemistry for optical properties of Si-ncs[27,28] and for their successful integration in application devices, our recent work has focused on viable methodologies for surface engineering without adding lengthy surfactants. In particular, we have studied different approaches that allow for three-dimensional surface engineering of Si-ncs directly in solution: the first technique is based on ns-laser processing and the second one on a direct-current (DC) atmospheric-pressure plasma treatment through plasma-induced liquid chemistry.[10,29,30] Both techniques have produced promising results that allow tuning the surface chemistry, providing a uniform passivation layer without using any lengthy surfactants that could hinder or complicate carrier dissociation and transport, as required for PV devices.[30]

Dr. V. Svrcek, Dr. K. Matsubara, Prof. M. Kondo
Research Center for Photovoltaics
National Institute of Advanced Industrial Science and Technology (AIST)
Central 2, Umezono 1–1–1, Tsukuba, 305–8568, Japan
E-mail: vladimir.svrcek@aist.go.jp
Dr. K. Dohnalova, Dr. M. T. Trinh,[+] Dr. R. Limpens, Prof. T. Gregorkiewicz
Van der Waals-Zeeman Institute
Science Park 904, 1098 XH Amsterdam, The Netherlands
Dr. D. Mariotti, S. Mitra
Nanotechnology & Integrated Bio-Engineering Centre (NIBEC)
University of Ulster, UK
[+]Present address: Department of Chemistry, Columbia University, New York, NY 10027, USA

DOI: 10.1002/adfm.201301468

In this manuscript, we report on a dramatic improvement of absolute photoluminescence (PL) quantum yields (QYs) for surfactant-free Si-ncs due to surface engineering by atmospheric pressure DC microplasma. Furthermore, given the critical role predicted for the Si-ncs surface in CM mechanisms, presence of CM is also investigated. Two different mechanisms, multiple exciton generation (MEG)[31] and space separated quantum cutting (SSQC),[16] are considered. MEG refers to a process in which multiple excitons are generated in the same nanocrystal (NC), hence Auger recombination will take place,[31] and SSQC refers to a process in which multiple excitons are generated in adjacent NCs and, therefore, Auger recombination is absent.[18] We report results of the investigations of the fast dynamics (measured by transient induced absorption) and corresponding measurements of the absolute PL-QY. We show that, for energy photons (2.3–3 eV) within the solar spectrum, the QY of surface-engineered Si-ncs is stabilized and improved by a factor of 120; specifically, the QY increases from 0.1% to 12% compared to as-prepared Si-ncs. Si-ncs properties remain stable with similar QY when stored in ethanol at ambient conditions for three months.

2. Surfactant-Free 3D-Surface Engineered Si-ncs

We have previously studied in detail the effect of the microplasma process on the surface characteristics of the Si-ncs, including the chemical changes in Si-ncs dispersed in ethanol and water.[10,29] Here, we summarize our previous findings to facilitate the discussion on QYs and CM mechanisms that will follow. As largely reported in the literature, Si-ncs produced by the electrochemical etching are mostly terminated by hydrogen ($Si–H_x$) and, at the same time, Si-dimers and dangling bonds are also present. Exposure to air, and in particular to gas-phase molecular oxygen and water vapors, causes Si-ncs oxidation. Spontaneous room temperature oxidation in air is expected to leave the Si–H bonds unaffected, as these would require high temperature to desorb (>500 °C), and therefore oxidation proceeds through passivation of dangling bonds or by breaking Si–Si bonds in Si-dimers or in silicon back-bonds. The effect of the oxidation by the water included in air is reduced due to the hydrophobic nature of the H-terminations, which also prevents replacement of the Si–H with the Si–OH. The result is a surface dominantly terminated by hydrogen atoms, where about a monolayer of oxide has been grown in the back-bonds of surface silicon, that is, $O_xSi–H_{4-x}$.

The introduction of Si-ncs powder into ethanol accelerates the oxidation process due to water (that dissolves in ethanol from the atmosphere), which generally proceeds differently from the oxidation in air, contributing to further inward oxide growth. This is confirmed by the Fourier transform IR spectroscopy (FTIR) transmission; specifically, in our samples we can observe the peak at 465 cm^{-1}, a small peak at 800 cm^{-1}, and a broad strong signal around 1060 cm^{-1} corresponding to the rocking, bending, and stretching modes of the Si–O–Si bonds, respectively.[10] Another interesting observation on the as-prepared Si-ncs is that $Si–H_x$ peaks with no oxygen back-bonds are predominantly due to $Si–H_3$ terminations.

The surface chemistry activated by microplasma in ethanol is to be due to multiple factors indeed mainly determined by the electrons injected from the microplasma into the colloidal Si-ncs/ethanol solution.[10,15] Electrons from the microplasma are injected through the plasma/colloid interface forming a liquid volume with very high electron densities ($\approx 10^{19}$ m^{-3}) inducing highly non-equilibrium kinetically driven reactions that would not be achievable in standard electro-chemistry or by radiolysis techniques.[32] Then, enhanced density, together with high kinetic energy of the electrons, induces surfactant-free chemical reactions at Si-ncs surface.[10,29] After the microplasma processing, all peaks corresponding to the H-related terminations are drastically reduced or completely removed (862 cm^{-1}, 875 cm^{-1}, 935 cm^{-1}, and 2070–2250 cm^{-1}). Importantly, the narrowing and strengthening of the Si–O in-phase contribution around 1050–1150 cm^{-1} is a strong indication of the replacement of H-terminations with Si–OR.[33,34] This is because the surface silicon atoms are now found within a complete set of oxygen bonds between the back-bonds oxide monolayer and the –OR terminations, and therefore, the surface arrangement exhibits characteristics close to that of a stochiometric oxide.[10] The broad signal around 3000–3600 cm^{-1} due to the OH is changed after microplasma processing with the appearance of a peak at 3740 cm^{-1}, attributed to the isolated non-hydrogen bonded Si-OH.[29] This may indicate that some of the H-terminations are also replaced by the OH ions, or possibly due to the OH present in the Si–OR compound. To complete the analysis, it should be noted that the microplasma-treated Si-ncs do not show any absorption related to the Si-C bonds (≈1258 cm^{-1} and 1273 cm^{-1})[35,36] or peaks attributed to C_xH_y compounds of the Si–OR terminations (at 1350–1450 cm^{-1} and 2900–3000 cm^{-1}).[35–37]

3. Multiple-Exciton Generation in Si-ncs

The CM phenomenon in the Si-ncs has been ascribed to MEG[31] and/or SSQC,[16] with each mechanism determined by a different excitons dynamics.[16,17] A widely used approach to investigate MEG is based on the measurements of the fast decay dynamics of the multiple exciton population in the nanocrystals, caused by the Auger recombination. The generation and detection of the multiple excitons is achieved by the time-resolved pump and probe measurements.[6] As a result, the evidence for the MEG comes from occurrence of ultrafast dynamics at high pump photon energies and low fluxes.[6,38]

The Si-ncs used in this work exhibit a strong room temperature PL, peaking around 2 eV, which is used here as the average optical bandgap $\approx E_g$ value.[10,30] We note that during the surface engineering by the DC microplasma treatment, the PL intensity of the Si-ncs is considerably increased and stabilized. At the same time, the PL maximum position red-shifts, probably due to changes in surface chemistry.[10,15,39] To avoid strong absorption from the solvent, the excitation photon energies were chosen to be below 5 eV, where the ethanol absorption is negligible (**Figure 1**). Both, the PL and the absorption analysis allow us to determine the minimal MEG energy threshold of $2E_g$, which is expected to be in our sample at ≈4 eV. The MEG is therefore investigated at the excitation photon energy E_{exc} = 4.66 eV, which is ≈2.3 E_g. For the reference, we also excite sample below the minimal MEG threshold at ≈1.55 E_g

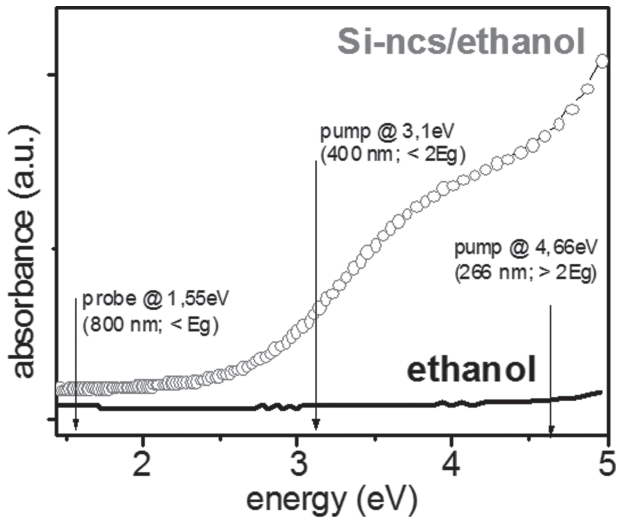

Figure 1. Typical absorption spectrum of the microplasma surface-engineered (for 90 min) Si-ncs in ethanol (circles). Both excitation and probe photon energies used in the pump and probe experiments are indicated by arrows. The absorbance for ethanol is also shown for comparison (black line).

(E_{exc} = 3.1 eV). The probe photon energy is chosen as less than E_g (E_{probe} = 1.55 eV, i.e., ≈0.78 E_g), to avoid direct excitation of carriers by the probe beam. In the transient induced absorption measurements, the excitation photon energies and the probe photon energy are indicated by arrows in the Figure 1.

In order to ensure a low-flux regime, that is, that no more than a single photon is absorbed in each Si-nc, we measured the decay dynamics at two different excitation powers. **Figure 2**a shows the decay dynamics of the as-prepared Si-ncs dispersed in ethanol at the excitation photon energy of 3.1 eV (1.55 E_g) for two excitation powers of 2 and 4 mW. It has to be noted that the data may look noisy because the induced absorption signal is relatively low. The reasons for the low transient absorption signal are multiple; low pump fluence, low absorption cross-section and low concentration of the Si-ncs. In order to avoid the absorption of multiphotons (that creates the trivial multiple excitons per Si-ncs), we kept the number of absorbed photons per Si-ncs at low fluence. As can be seen, the transient decay dynamics are independent of the excitation power, that is, there is no onset of the Auger recombination as an addition of a fast decay at a short time scale. The lower pump power of 2 mW can be therefore safely used as the single-exciton excitation regime.[28] The overall decay at 1 ns time scale was attributed to trapping and/or charge transfer.[31,40] To find out, whether MEG is present in our sample, we compare the induced absorption signals for excitation energies below and above the CM threshold of $2E_g$. At the low pump flux regime.

The results are presented in Figure 2b, which shows the same decay characteristics at photon energies below and above the $2E_g$ threshold, corresponding to 3.1 eV (1.55 E_g) and 4.66 eV (2.3 E_g), respectively. As can be seen, there is no fast component appearing at the excitation energies above the CM threshold, implying no Auger interaction of multiple excitons in a single NC. We conclude that no signature of MEG has been observed for 4.66 eV (2.3 E_g) excitation photon energy. The rise in the

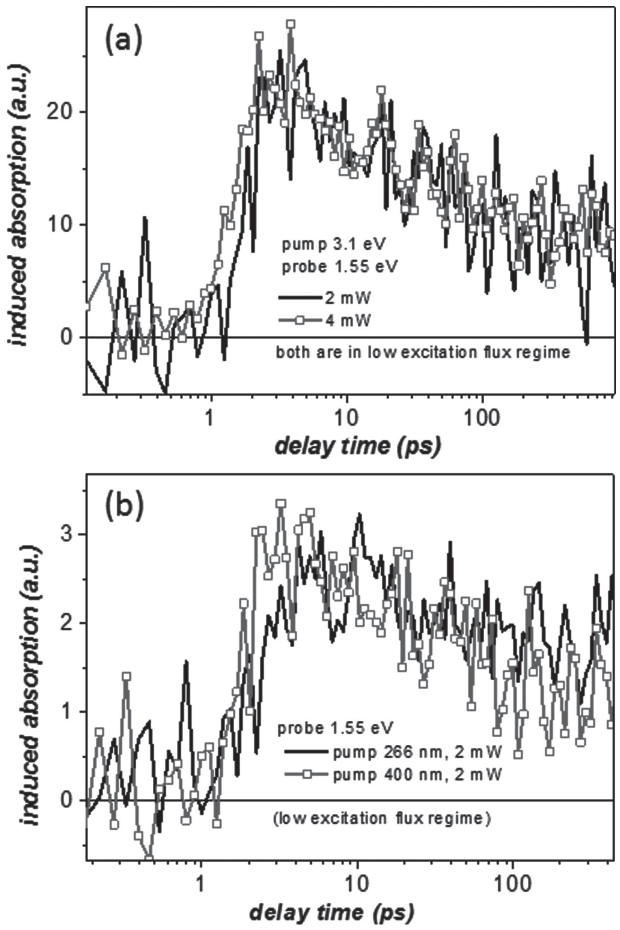

Figure 2. a) Induced absorption dynamics of as-prepared silicon nanocrystals in ethanol for two fluxes, at 2 mW and 4 mW. b) Comparison of the induced absorption dynamics after excitation below and above the MEG threshold (pump <$2E_g$ and >$2E_g$) at 2 mW pump power.

first few picoseconds reflects the cross-correlation between pump and probe pulses. This rising time is depending on the difference in wavelengths of pump and probe pulses (different speed of light in the solution) and the thickness of the sample cuvette. It is clear to see that the rise for 4.66 eV excitation is slower than that of 3.1 eV excitation, due to a larger difference in pump and probe energy for 4.66 eV.

Subsequently, we have surface-treated the Si-ncs by DC microplasma, as described in the experimental section. **Figure 3** shows the PL spectra of Si-ncs in ethanol before and after microplasma treatment. A clear increase of PL intensity (>12 times) is observed for the microplasma-treated Si-ncs with an obvious red-shift of the PL maximum from 2.16 eV to 1.9 eV. This is the result of multiple mechanisms induced by the microplasma process and due to electron-driven non-equilibrium liquid chemistry[10,29,41] that follows unique reaction paths for termination and passivation of the Si-ncs surface. As mentioned above, the analysis of the Si-ncs surface properties by FTIR revealed that the microplasma surface engineering produces the single-bonded Si–O terminations such as in Si–OH that reduce the energy band gap and lead to a PL red-shift.[10] On the other hand, the microplasma process induces a

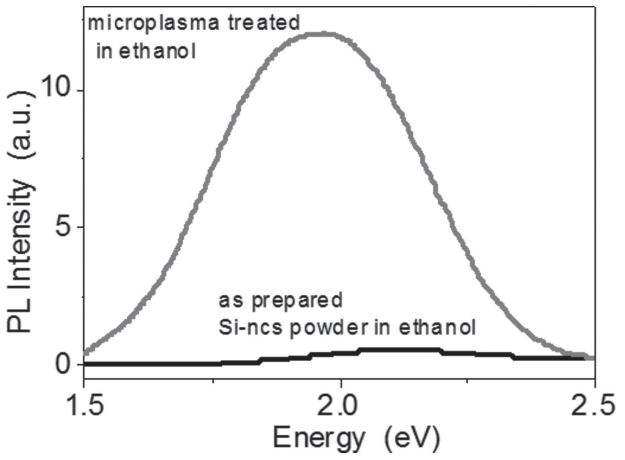

Figure 3. PL spectra of as-prepared (black line, lower intensity) Si-ncs and for Si-ncs after microplasma processing in ethanol (grey line, higher intensity).

surface-restricted modification without affecting the core of the Si-ncs, so that the size distribution also remained unchanged after surface engineering; this can be observed in the full width at half maximum of the PL emission (1.1 eV) which is about the same for both spectra in Figure 3.

We now analyze the effect of the surface chemistry on the dynamics of the generation–recombination processes. The induced absorption dynamics after microplasma-induced 3D surface engineering (**Figure 4**) did not show significant differences compared to the measurements of as-prepared Si-ncs (Figure 2). Figure 4a,b show the decay dynamics for microplasma-treated Si-ncs in ethanol at different pump powers for two different pump photon energies of 4.66 and 3.1 eV, respectively. Probing energy was always set at 1.55 eV. As can be seen, there is no difference in dynamics for different pump powers, again indicating of sufficient low pump power to avoid the absorption of multiple photons at these pump regimes. Figure 4c presents the decay dynamics for two different pump energies (below and above the MEG threshold of $2E_g$) at the low pump powers. It is shown that the decay dynamics at 4.66 eV excitation is not faster than that at 3.1 eV excitation, which indicates that Auger recombination does not occur, even at the high pump photon energy (2.45 E_g).[42] This confirms that no CM through MEG processes occurs even after Si-ncs surface engineering. On the other hand, the decay dynamics investigations within single Si-ncs also support the idea that the core of the Si-ncs was not affected and that the chemistry induced by microplasma processing was restricted to the Si-ncs surfaces.[29]

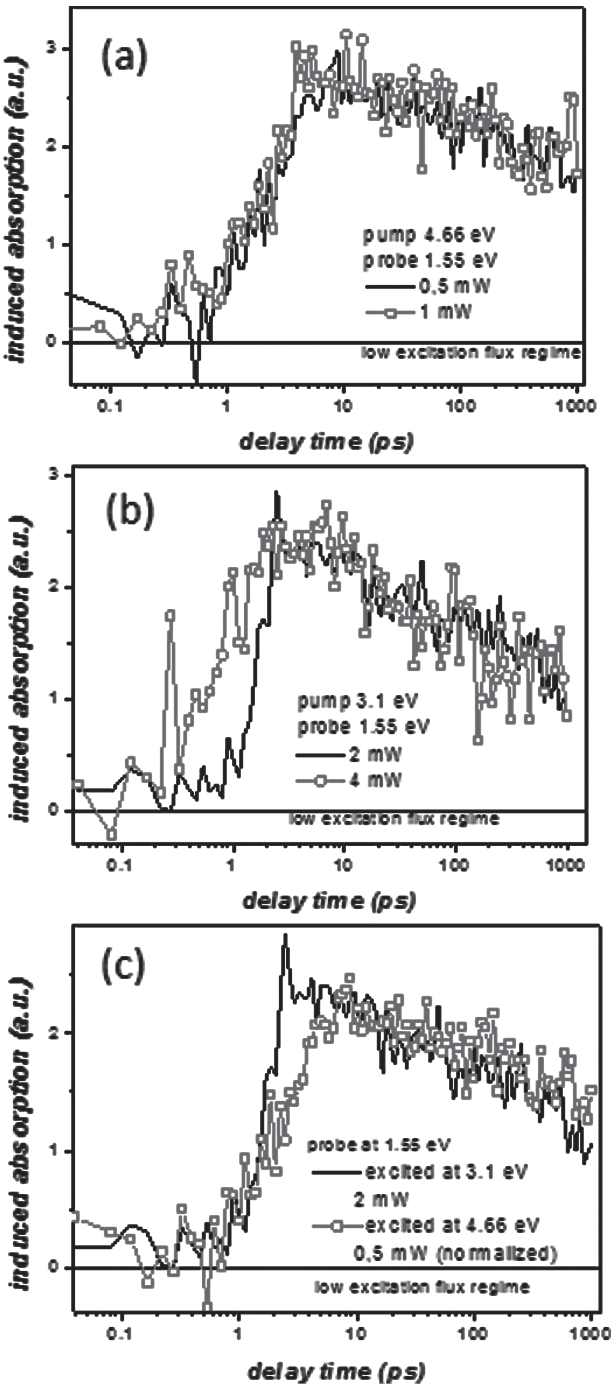

Figure 4. a) Induced absorption dynamics of microplasma-engineered silicon nanocrystals in ethanol for two powers (0.5 mW and 1 mW) of pumping and probe photon energy of 1.55 eV. b) Induced absorption dynamics for two powers (2 mW and 4 mW) of pumping power with photon energy of 3.1 eV and probe photon energy of 1.55 eV. c) Comparison of induced absorption dynamics for excitation below and above the multi-exciton generation threshold ($<2E_g$ and $>2E_g$) at the low pump fluxes. All dynamics were probed at 1.55 eV.

4. Carrier Multiplication in Si-ncs Through the Space Separated Quantum Cutting Effect

SSQC can be investigated by measurements of the QY as a function of pump photon energy. Since the PL can only be accounted for a long-live excitons, all single-excited NCs are considered, which can appear due to direct photon absorption or as a result of the SSQC process. In SSQC, exciton separation occurs across neighboring nanocrystals, suppressing interactions between multiple carriers.[16,18] Since multiple excitons are excited within separated Si-ncs, their lifetimes correspond to the single exciton lifetime (μs).[43–45] In our case, the evaluation of the PL

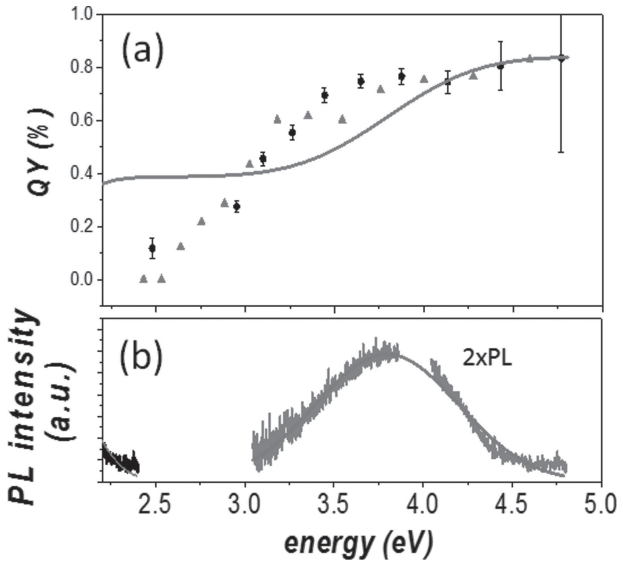

Figure 5. a) Dependence of the photoluminescence (PL) quantum yield (QY) on the excitation photon energy for the as-prepared silicon nanocrystals dispersed in ethanol (black circles); grey triangles correspond to measurements on the same sample after three months. The red curve represents theoretical model for the SSQC.[17] b) For reference, the energy doubled PL spectrum of the same sample is also included (i.e., the energy axis is multiplied by 2).

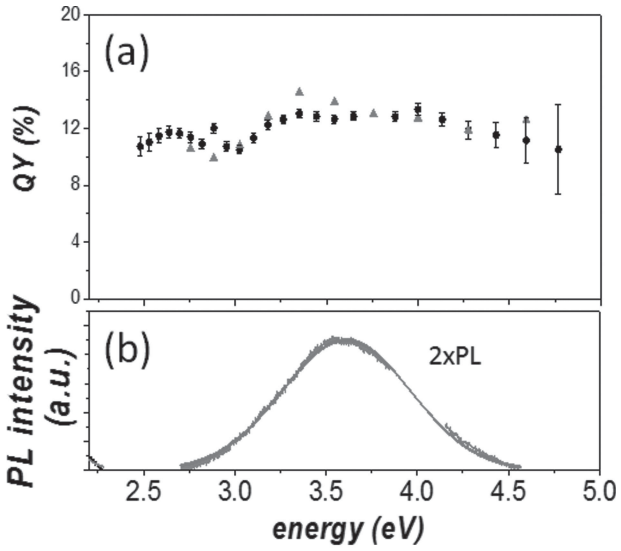

Figure 6. a) Dependence of the photoluminescence (PL) quantum yield on excitation photon energy for the microplasma-treated Si-ncs dispersed in ethanol (black circles); the red triangles correspond to measurements taken after three months. b) For reference, the PL spectra at multiples of the PL peak is also included (i.e., the energy axis is multiplied by 2).

decay constant reveals a characteristic lifetime of about ≈25 μs. Studies[18,42] have shown that an increase of induced absorption intensity (normalized to the number of absorbed photons), in combination with the absence of Auger-related components in the dynamics, can evidence that CM occurs at high pumping photon energy, but however does not lead to interaction between the generated carriers. Because the multiple carriers in Si-ncs, as a result of SSQC, are not destroyed by the non-radiative Auger recombination, they contribute to PL and can be monitored by enhancement of PL QY.[17,46]

Figure 5a shows the dependence of the PL QY on the excitation photon energy for the as-prepared Si-ncs in ethanol (black circles). The corresponding lower panel (Figure 5b) shows the PL spectrum with the doubled energy values for reference. The increasing trend of the QY might be indication of presence of the SSQC effect.[17] In principle, in our sample of as-prepared Si-ncs this could occur within Si-ncs aggregates present in the solution. However, CM onset is expected to occur at 2 E_g, that is, around 3.5 eV (see Figure 5a, red line), suggesting that increase in QY might be of different origin. It is important to notice that the Si-ncs are stable in ethanol and after three months the same increase in QY is recorded (red triangles in Figure 5a). However, when we compare our experimental results with the theoretical model (red line in Figure 5a) the experimental data do not follow the model curve. In fact, the experimental data show that the increase in QY is observed for low energy values (≈2.5 eV) while the model and theory suggests that the threshold should be at $2E_g$, that is, above 3.5 eV in our case (Figure 5b).

Figure 6a shows the PL QY for the microplasma-treated Si-ncs in ethanol (black circles) and re-measured after three months of aging in ethanol (red triangles). The lower panel (Figure 6b) reports PL spectra at two times PL peak for reference. After surface-engineering, the QY has drastically increased, compared to as-prepared Si-ncs (Figure 5a) and in this case the QY remains nearly constant around ≈12% across a large excitation region (2.5–4.5 eV); this sample also shows long-term stability (>3 months) with respect to the QY (red triangles in Figure 6a). The constant trend of the QY as a function of photon excitation energy indicates the absence of any SSQC evidence for these surface-treated Si-ncs. The possible origin of the rise in the QY of as-prepared sample could be cause by large amount of non-emitting materials (such as bulk silicon pieces in mechanically scraped porous Si aggregates) with spectrally shifted absorption spectrum (with respect to the Si-ncs). This could also partially contribute to the enhancement of the QY in plasma treated sample.

5. Quantum Yield of 3D Surface-Engineered Si-ncs within the Solar Spectrum

The TEM image in **Figure 7**a shows a typical aggregated structure of as-prepared Si-ncs which suggests that Si-ncs are closely spaced. On the contrary, the TEM images of Figure 7b show that the surface modification by microplasma treatment induces Si-ncs separation. We can speculate that the Si-ncs separation induced by the microplasma-treatment as seen in **Figure 8**b may have contributed to the reduction of SSQC. This is because the SSQC requires close proximity of neighboring Si-ncs for efficient energy transfer and, therefore, nanostructured arrangements of closely packed Si-ncs are preferable.[17]

Figure 8 compares the solar spectrum intensity and the absolute QY as a function of the excitation photon energy for as-prepared Si-ncs dispersed in ethanol and microplasma-treated Si-ncs in ethanol. Our results clearly show that the PL QY is enhanced by ≈15 times (from 0.8% to 12%) for high-energy

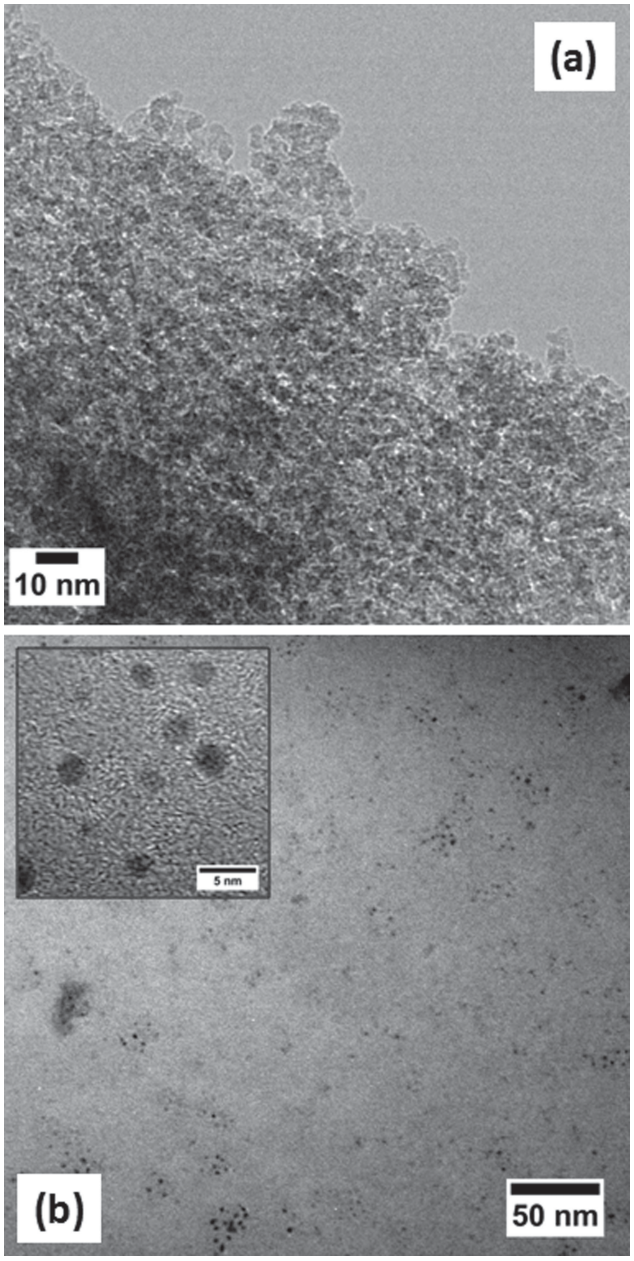

Figure 7. Transmission electron microscope images of a) as-prepared and b) surface-engineered Si-ncs. Inset in (b) shows the Si-ncs in detail (bar is 5 nm).

excitation (3.5–4.8 eV) while for low-energy photons (<2.7 eV) the QY increase is considerable, from ≈0.1% to 12%, that is, more than 120 times enhancement. We can also observe that the energy ranges with QY enhancement overlap significantly with a spectral region which has relevance for photovoltaic applications. Overall our results (e.g., dynamics in single Si-ncs) showed that the core structure was not modified by the microplasma process. Therefore surface-engineered and surfactant-free Si-ncs with high QY could in principle be arranged on substrates in close-packed structures that allow the Si-ncs to be sufficiently close to each other for SSQC to occur (it should be noted that our SSQC measurements were performed with

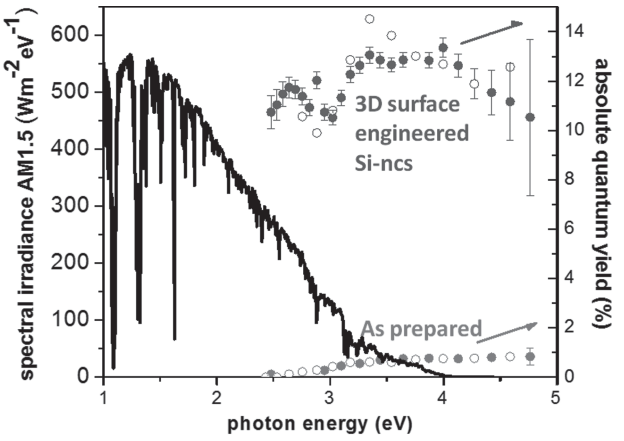

Figure 8. Solar spectral irradiance for AM 1.5 (black line, left axis) and absolute quantum yield (QY) as a function of excitation photon energy for as-prepared Si-ncs dispersed in ethanol (full light-grey circles) and microplasma-treated Si-ncs also in ethanol (full dark-grey circles). Open symbols represent corresponding QY after aging in ethanol for three months.

the Si-ncs in low-density colloids). Furthermore, the absence of long ligands in the microplasma-treated Si-ncs could be highly beneficial for the carrier transport, required for the PV devices.

6. Summary

Dramatic improvements in the absolute PL QY of surfactant-free 3D surface-engineered Si-ncs within an important spectral region are demonstrated. The microplasma-induced 3D surface engineering results in more than 120 times enhancement QY for low energy photons (<2.7 eV) and ≈15 times higher for high energy photons (3.5–4.8 eV). Furthermore, QY measurements have confirmed that microplasma-treated Si-ncs present well-passivated surface characteristics with a stable QY enhancement for several months.

Since CM can considerably improve solar cells performance, we have investigated CM mechanisms in both as-prepared and surface-treated Si-ncs. Specifically, CM through MEG and SSQC has been considered. In the current study, we could not confirm the presence of CM either by MEG or SSQC, although some indirect evidence of CM has been found, but with strongly red-shifted onset of the step-like QY behavior for the as-prepared Si-ncs. The excitation dependence of PL QY was strongly modified by the microplasma treatment, possibly due to improved dispersion of the surface-treated Si-ncs. It is believed that the formation of closely-packed microplasma-treated Si-ncs on substrates could eventually lead to Si-ncs films with high QY and where SSQC may be possible due to the closer proximity of Si-ncs. Further work in this direction is necessary to provide valuable opportunities for integrating Si-ncs in solar cell devices.

7. Experimental Section

In this study, the Si-ncs were produced by electrochemical etching of a silicon wafer (p-type boron doped, <100>, 0.1 Ω cm, thickness 0.525 mm) and subsequent mechanical pulverization.[47] The process produces a dry powder of Si-ncs with diameter of 3–5 nm which generally includes Si-ncs aggregates of different sizes up to the micrometer range. The Si-ncs

powder was then stored in glass containers in ambient conditions and exposed to air. Afterwards, ≈3 mg of the powder was dispersed in 10 mL of ethanol before being processed by a DC microplasma treatment. The microplasma treatment was conducted similarly to our previous work:[10] a DC atmospheric-pressure microplasma was generated between a Ni tubing (inner diameter 0.7 mm, outer 1 mm) and the surface of the Si-ncs colloid. As a counter electrode, a carbon rod (5 mm diameter) was immersed about 5 mm in the colloid at a distance of about 3 cm from the nickel tubing. A positive voltage was applied to the carbon rod, while the Ni tubing was connected to ground through a 100 kΩ resistor. Pure argon was flown inside the Ni tubing at a rate of 25 sccm. The distance between the Ni tubing and the liquid dispersion surface was initially adjusted at 1 mm, however during processing the distance was observed to increase to about 1.3–1.5 mm (about every ≈15 min of processing) due to evaporation. The temperature of the colloids did not increase above 38 °C within ≈15 min processing time. During the microplasma treatment, the conductivity of the colloid was also observed to change.[10] For this reason, the applied voltage was initially set at 2 kV until the current reached 1.5 mA and later adjusted to keep the current constant at this value. The Si-ncs is then dissolved in methanol in a quartz cuvette with a path length of 1 cm for measurements. CM (refers to both MEG and SSQC) was assessed in the Si-ncs utilizing a conventional pump-probe setup that allowed MEG measurements. The experimental setup was described in previous work,[30] which used a femtosecond pulse from a chirped-pulse amplified Ti:sapphire laser system, which runs at 1 kHz and delivers pulses of 60 fs, 2.2 mJ, at 795 nm wavelength. Dimensions of the pump spot size were chosen to be considerably larger than probe size to assure complete overlap during the entire experiment. The probe photon energy was set at E_{probe} = 1.55 eV which is below the optical bandgap of Si-ncs. The pump photon energies were 3.10 eV and 4.65 eV. All the measurements were carried out at room temperature. For measurements of PL QY, an integration sphere was used to collect the PL of the Si-ncs colloida. For the excitation, a Xe lamp with a double monochromator was used, and the PL was detected by a charge-coupled detector (CCD) mounted on a spectrograph via coupled ultraviolet-grade optical fiber. The excitation wavelength was selected through the monochromator. At each step, both the emission spectra from the sample (Si-ncs in ethanol) and the reference (ethanol only) were measured, and the number of emitted photons was then calculated from spectral integration. The number of absorbed photons was calculated using reduction of the excitation spectrum comparing sample and reference. The absolute QY is obtained as the ratio of the number of emitted photons to the number of absorbed photons.[17,46] The PL spectra of the Si-ncs in colloidal were measured with Spectrofluorometer (FluoroMax-4) at 400 nm excitation. Transmission electron microscope (TEM) images were taken with a Hitachi S-4300 microscope at 20 kV after the colloid was drop-casted on TEM grids.

Acknowledgements

K.D. and R.L. measured QY, M.T.T. measured IA. V.S. has prepared the samples, measured PL, made the model and interpreted the data. All authors contributed to discussion and written the paper. This work was partially supported by a NEDO project and FOM (Stichting voor Fundamenteel Onderzoek der Materie), NanoNext, and the Technology Foundation STW. The TEM analysis was supported by the Science Foundation Ireland National Access Programme (Project n. 283). D.M. acknowledges the support of the JSPS Invitation Fellowship, JSPS Bridge Fellowship, the University of Ulster Strategic Research Fund, the Leverhulme International Network on "Materials processing by atmospheric pressure plasmas for energy applications" (Award n.IN-2012–136) and by the Royal Society International Exchanges scheme (Award n.IE120884). S.M. thanks the financial support of the University of Ulster Vice-Chancellor Studentship. The authors thank J. M. Schins and L. D. A. Siebbeles for facilitating femtosecond experiments.

Received: April 30, 2013
Revised: June 6, 2013
Published online: July 2, 2013

[1] H. O. Jacobs, A. R. Tao, A. Schwartz, D. H. Gracias, G. M. Whiesites, *Science* **2002**, *296*, 323.
[2] J. P. Desai, A. Pillarisetti, A. D. Brooks, *Annu. Rev. Biomed. Eng.* **2007**, *9*, 35.
[3] D. J. Maxwell, J. R. Taylor, S. M. Nie, *J. Am. Chem. Soc.* **2002**, *124*, 9606.
[4] A. Badolato, K. Hennessy, M. Atature, J. Dreiser, E. Hu, P. M. Petroff, A. Imamoglu, *Science* **2005**, *308*, 1158.
[5] A. Jamshidi, P. J. Pauzauskie, P. J. Schuck, A. T. Ohta, P. Y. Chiou, J. Chou, P. D. Yang, M. C. Wu, *Nat. Photonics* **2008**, *2*, 85.
[6] R. D. Schaller, V. I. Klimov, *Phys. Rev. Lett.* **2004**, *92*, 186601.
[7] J. A. Fan, K. B. Bao, R. Bardhan, N. J. Halas, V. N. Manoharan, P. Nordlander, F. Capasso, *Science* **2010**, *328*, 1135.
[8] J. A. Smyder, T. D. Krauss, *Mater. Today* **2011**, *14*, 382.
[9] R. Bardhan, N. Grady, T. Ali, N. J. Halas, *ACS Nano* **2010**, *4*, 6169.
[10] V. Švrcek, D. Mariotti, M. Kondo, *Appl. Phys. Lett.* **2010**, *97*, 161502.
[11] A. Hoshino, K. Fujioka, T. Oku, M. Suga, Y. F. Sasaki, T. Ohta, M. Yasuhara, K. Suzuki, K. Yamamoto, *Nano Letters* **2004**, *4*, 2163.
[12] J. A. McGuire, M. Sykora, J. Joo, J. M. Pietryga, V. I. Klimov, *Nano Lett.* **2010**, *10*, 2049.
[13] B. G. Streetman, S. Banerjee, *Solid State Electronic Devices*, 5th ed., Prentice Hall, New Jersey, **2000**.
[14] A. J. Nozik, *Chem. Phys. Lett.* **2008**, *457*, 3.
[15] D. Mariotti, M. Somak, V. Švrcek, *Nanoscale* **2013**, *5*, 1385.
[16] D. Timmerman, I. Izeddin, P. Stallinga, I. N. Yassievich, T. Gregorkiewicz, *Nat. Photonics* **2008**, *2*, 105.
[17] D. Timmerman, J. Valenta, K. Dohnalová, W. D. A. M. de Boer, T. Gregorkiewicz, *Nat. Nanotechnol.* **2011**, *6*, 710.
[18] M. T. Trinh, R. Limpens, W. D. A. M. de Boer, J. M. Schins, L. D. A. Siebbeles, T. Gregorkiewicz, *Nat. Photonics* **2012**, *6*, 316.
[19] W. Shockley, H. J. Queisser, *J. Appl. Phys.* **1961**, *32*, 510.
[20] V. I. Klimov, *Appl. Phys. Lett.* **2006**, *89*, 123118.
[21] A. Franceschetti, J. M. An, A. Zunger, *Nano Lett.* **2006**, *6*, 2191.
[22] A. Shabaev, Al. L. Efros, A. J. Nozik, *Nano Lett.* **2006**, *6*, 2856.
[23] G. Nair, M. G. Bawendi, *Phys. Rev. B* **2007**, *76*, 081304.
[24] J. J. H. Pijpers, E. Hendry, M. T. W. Milder, R. Fanciulli, J. Savolainen, J. L. Herek, D. Vanmaekelbergh, S. Ruhman, D. Mocatta, D. Oron, A. Aharoni, U. Banin, M. Bonn, *J. Phys. Chem. C* **2008**, *112*, 4783.
[25] M. Ben-Lulu, D. Mocatta, M. Bonn, U. Banin, S. Ruhman, *Nano Lett.* **2008**, *8*, 1207.
[26] A. J. Nozik, *Phys. E* **2002**, *14*, 115.
[27] G. Allan, C. Delerue, *Phys. Rev. B* **2009**, *79*, 195324.
[28] M. T. Trinh, A. J. Houtepen, J. M. Schins, T. Hanrath, J. Piris, W. Knulst, A. P. Goossens, L. D. Siebbeles, *Nano Lett.* **2008**, *8*, 1713.
[29] D. Mariotti, V. Švrcek, W. J. Hamilton, M. Schmidt, M. Kondo, *Adv. Funct. Mater.* **2012**, *22*, 954.
[30] V. Švrcek, D. Mariotti, T. Nagai, Y. Shibata, I. Turkevych, M. Kondo, *J. Phys. Chem. C* **2011**, *115*, 5084.
[31] M. C. Beard, K. P. Knutsen, P. Yu, J. M. Luther, Q. Song, W. K. Metzger, R. J. Ellingson, A. J. Nozik, *Nano Lett.* **2007**, *7*, 2506.
[32] B. H. Milosavljevic, O. I. Micic, *J. Phys. Chem.* **1987**, *82*, 1360.
[33] N. Y. Kim, P. E. Laibinis, *J. Am. Chem. Soc.* **1999**, *121*, 7162.
[34] D. J. Amy, D. Aureau, M. Dai, A. Esteve, Y. J. Chabal, *Nat. Mater.* **2010**, *9*, 266.
[35] D. Xu, L. Sun, H. Li, L. Zhang, G. Guo, X. Zhao, L. Gui, *New J. Chem.* **2003**, *27*, 300.
[36] K. Kusová, O. Cibulka, K. Dohnalova, I. Pelant, J. Valenta, A. Fucikova, K. Zidek, J. Lang, J. Englich, P. Matejka, P. Stepanek, S. Bakardjieva, *ACS Nano* **2010**, *4*, 4495.
[37] A. Grill, D. A. Neumayer, *J. Appl. Phys.* **2003**, *94*, 6697.
[38] N. M. Gabor, Z. H. Zhong, K. Bosnick, J. Park, P. L. McEuen, *Science* **2009**, *325*, 1367.
[39] V. Švrcek, D. Mariotti, Y. Shibata, M. Kondo, *J. Phys. D: Appl. Phys.* **2010**, *43*, 415402.
[40] M. T. Trinh, R. Limpens, T. Gregorkiewicz, *J. Phys. Chem. C* **2013**, *117*, 5963.

[41] D. Mariotti, R. M. Sankaran, *J. Phys. D: Appl. Phys.* **2010**, *43*, 323001.
[42] W. D. A. M. de Boer, M. T. Trinh, D. Timmerman, J. M. Schins, L. D. A. Siebbeles, T. Gregorkiewicz, *Appl. Phys. Lett.* **2011**, *99*, 053126.
[43] D. Timmerman, I. Izeddin, T. Gregorkiewicz, *Phys. Status Solidi A* **2010**, *1*, 183.
[44] M. L. Brongersma, A. Polman, K. S. Min, E. Boer, T. Tambo, H. A. Atwater, *Appl. Phys. Lett.* **1998**, *72*, 2577.
[45] V. Vinciguerra, G. Franzo, F. Priolo, F. Iacona, C. Spinella, *J. Appl. Phys.* **2000**, *87*, 8165.
[46] U. Kortshagen, *J. Lumin.* **2006**, *121*, 327.
[47] V. Švrcek, A. Slaoui, J.-C. Muller, *J. Appl. Phys.* **2004**, *95*, 3158.